Using Delayed Observations for Long-Term Vehicle Tracking in Large Environments

Mao Shan, *Member, IEEE*, Stewart Worrall, *Member, IEEE*, Favio Masson, *Member, IEEE*, and Eduardo Nebot, *Senior Member, IEEE*

***Abstract*—The tracking of vehicles over large areas with limited position observations is of significant importance in many industrial applications. This paper presents algorithms for long-term vehicle motion estimation based on a vehicle motion model that incorporates the properties of the working environment and information collected by other mobile agents and fixed infrastructure collection points. The prediction algorithm provides long-term estimates of vehicle positions using speed and timing profiles built for a particular environment and considering the probability of a vehicle stopping. A limited number of data collection points distributed around the field are used to update the estimates, with negative information (no communication) also used to improve the prediction. This paper introduces the concept of observation harvesting, a process in which peer-to-peer communication between vehicles allows egocentric position updates to be relayed among vehicles and finally conveyed to the collection point for an improved position estimate. Positive and negative communication information is incorporated into the fusion stage, and a particle filter is used to incorporate the delayed observations harvested from vehicles in the field to improve the position estimates. The contributions of this work enable the optimization of fleet scheduling using discrete observations. Experimental results from a typical large-scale mining operation are presented to validate the algorithms.**

***Index Terms*—Delayed observations, intervehicle communication, long-term motion prediction, particle filtering, vehicle tracking.**

I. Introduction

ACCURATE tracking of vehicle positions is very important in applications such as traffic management, improving resource utilization, autonomous systems, vehicle safety, and many others. The standard approach to vehicle tracking is to have vehicles in direct communication with a centralized "control room" and broadcast the current state information. There are many applications where the infrastructure required to provide full communication coverage is not feasible due to a large area of operation, geographic constraints (terrain), etc. In most cases, however, it is possible to install a number of fixed data collection points and to fit a fleet of vehicles with vehicle-to-vehicle (V2V) communication capabilities. The data collection points are connected to a central base station or control room, providing a central location for scheduling and fleet management. In this case, V2V in combination with sparsely distributed vehicle-to-infrastructure (V2I) communication can be combined with vehicle models to obtain accurate prediction and tracking of the fleet. In addition, in [1], the V2V and V2I communication has been employed to improve the efficiency of traffic management.

There are various existing sensing technologies that can track the state (e.g., position, speed, and heading) of people or vehicles in an outdoor environment. In a typical tracking application, observations obtained from sensors are distributed among nearby vehicles, using some form of wireless communication such as ad hoc wireless sensor networks [2], vehicular mobile ad hoc networks [3], delay-tolerant networks (DTNs) [4], etc. In most applications, frequent measurements are required to reduce the uncertainty of the vehicle position. Most of the existing work in this area focuses on the tracking of vehicles in small areas. The complexity of the problem dramatically changes when the vehicle position estimates are required over a large environment of potentially hundreds of square kilometers.[1] This is further complicated in an environment with difficult terrain for communication purposes, such as a typical mountainous environment shown in Fig. 1. Deploying infrastructure to provide complete site-wide communication becomes very expensive, and consequently, it is only feasible to provide sparse coverage where vehicles may not be observed by a central control room for a long period of time. Generally, the uncertainty of the vehicle position quickly grows in the absence of position observations, and the vehicle position estimate becomes unusable after a short period of time.

This paper extends our previous work in [5], which presented a technique for long-term vehicle motion prediction and tracking based on a model of the vehicle that incorporates the known properties of the environment. It uses a limited number of data collection points distributed around the field to update vehicle position estimates when in range and then predict vehicle positions at points in between.

The current work introduces the concept of observation harvesting, where peer-to-peer (P2P) communication between vehicles allows position updates to be exchanged and brought

Manuscript received December 17, 2012; revised May 1, 2013 and August 8, 2013; accepted November 13, 2013. Date of publication January 2, 2014; date of current version May 30, 2014. The Associate Editor for this paper was H. J. W. C. Van Lint.

M. Shan, S. Worrall, and E. Nebot are with the Australian Centre for Field Robotics, The University of Sydney, Sydney, NSW 2006, Australia (e-mail: m.shan@acfr.usyd.edu.au; s.worrall@acfr.usyd.edu.au; nebot@acfr.usyd.edu.au).

F. Masson is with Consejo Nacional de Investigaciones Científicas y Técnicas, Instituto de Investigacion en Ingeniería Eléctrica "Alfredo Desages," Universidad Nacional del Sur, B8000CPB Bahia Blanca, Argentina (e-mail: fmasson@uns.edu.ar).

Color versions of one or more of the figures in this paper are available online at http://ieeexplore.ieee.org.

Digital Object Identifier 10.1109/TITS.2013.2292934

[1]Some types of mines, particularly where the resources to extract are not deep (e.g., bauxite mines), can extend for more than 100 km.

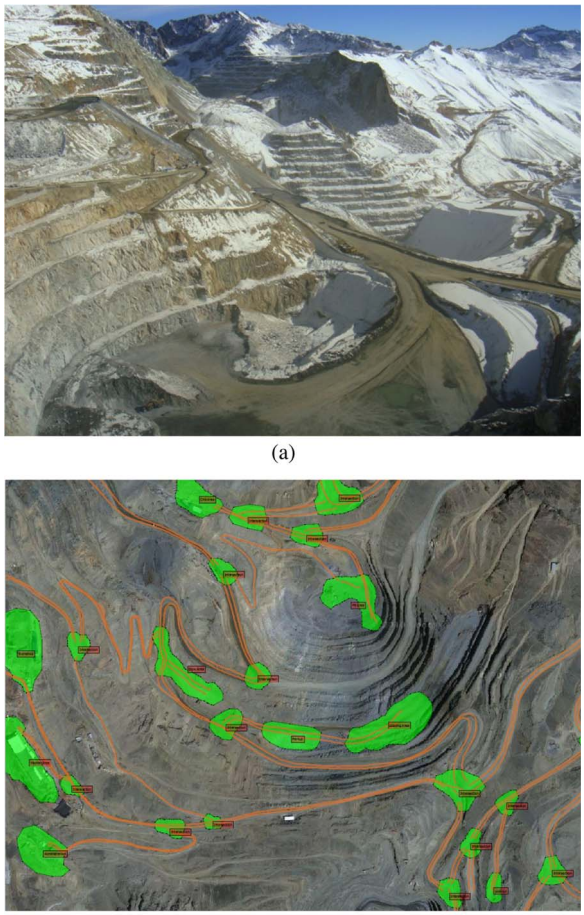

Fig. 1. Features in a mining operation. The mountainous environment illustrated in (a) can be represented by a road network based on context areas (loading areas, parking lots, etc.) connected by winding road segments and intersections formed by crossing roads, as demonstrated in (b).

forward to any of the fixed data collection points, which then connect through to the centralized base station. We introduce new algorithms to incorporate the delayed information into the global position estimate when a vehicle brings back information to a data collection point. Furthermore, the negative information from observers is also used in the fusion stage.

In summary, this paper extends our previous work toward long-term multivehicle motion prediction and tracking. Egocentric position information from vehicles not in the communication range of infrastructure is brought back to the central base station through intervehicle communication (the observation harvesting). The main contribution of this work is the introduction of a nonparametric filtering algorithm to fuse the delayed information collected during vehicle interactions. The algorithms are resilient to failures of fixed data collection points since the estimation of position based on the vehicle interactions can be downloaded by any vehicle and at any working data collection point.

The remainder of this paper is organized as follows. Section II describes the related work in the area of agent motion prediction and tracking. Section III presents a brief summary of the modeling of roads, intersections, and areas [5], followed by a probabilistic formulation of a long-term motion prediction algorithm. Following the observation harvesting mechanism introduced in Section IV, Section V proposes a probabilistic tracking algorithm to fuse the delayed information, as well as the implementation using a particle filter. Section VI presents experimental results of tracking multiple vehicles, followed by discussions. Lastly, conclusions and possible future work are presented in Section VII.

II. Related Work

Due to a complex interrelationship between vehicular and environmental variables, it is generally not feasible to explicitly parameterize the inherently nonlinear system process and measurement noise into a vehicle kinematic model [6]. Probabilistic approaches have been widely used for motion prediction making use of motion pattern learning techniques. These approaches predict the future state of a vehicle based on the assumption that the vehicle motion has typical patterns, which can be learned. To date, literature on vehicle tracking and motion prediction based on historical patterns mainly relies on an efficient pattern learning and recognition technique. More specifically, strongly related research areas are trajectory matching and trajectory classifiers. References [7] and [8] used hidden Markov models (HMMs) for vehicle and people tracking applications, respectively. An extension of the HMM given in [9] incrementally learns motion patterns online to predict vehicle motion. In [10] and [11], neural networks were trained with actual vehicle measurements to predict the future state of the vehicle given steering angle and velocity inputs. More work related to learning-driven approaches are surveyed in [12]. These existing approaches are capable of predicting vehicle motion up to a few seconds into the future, which is, however, far from the requirement of several minutes prediction addressed in this paper.

Cooperative localization has attracted a growing interest in the research community. In a noncooperative centralized localization scenario, only interactions between agents and infrastructure are incorporated into the position estimate. In a large environment, it is very difficult to guarantee that the wireless infrastructure can cover the entire working area, which reduces the performance of a global localization strategy. With cooperative localization, the communication between vehicles can reduce the need for all vehicles to be always within the range of centralized infrastructure. Reference [13] applied a cooperative approach to indoor localization with benefits demonstrated from the cooperation between agents. Similar work is presented in [14], where a decentralized cooperative approach is adopted, aiming for self-tracking in large mobile wireless networks. Interested readers may refer to [15]–[20] for more examples on cooperative localization.

In a standard cooperative framework, real-time vehicle state information can be transmitted to other vehicles using multihop communication through a mesh network [21]. However, an isolated agent problem occurs when there is segmentation of the mesh, which is inevitable in a large sparsely populated environment, as illustrated in Fig. 2(a). A possible solution to this problem is to use additional mobile agents that travel close to the isolated agent(s) to collect the state information updates and bring the information to the main network, although with some

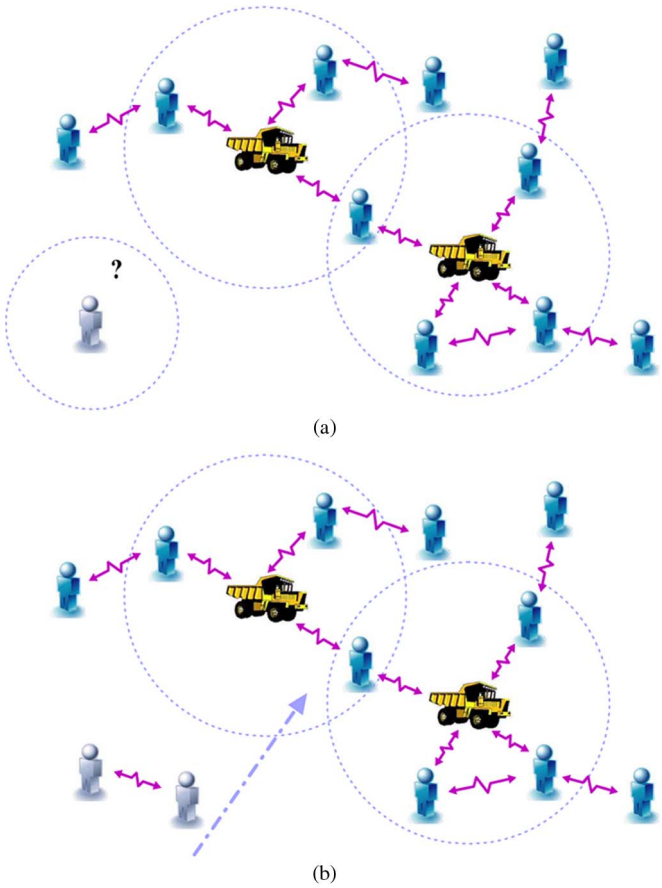

Fig. 2. Cooperative localization and the isolated agent issue. (a) Typical cooperative localization application where every agent (but one) is connected with others nearby to form a mesh network. An isolated agent problem occurs when an agent does not have any neighbors around and is consequently unable to join the mesh. In (b), another mobile agent passes and brings the information from the isolated agent, although delayed, back to the main mesh.

time delay. This approach requires a network that is capable of allowing time delays in data transmission and a filtering method capable of fusing the delayed information received.

DTNs are appropriate candidates for applications where continuous network connectivity is not available. A key difference between DTNs and traditional networks is that a traditional network requires a reliable end-to-end route to be established and maintained until the communication is completed. This is not a requirement for DTNs, which use store-and-forward-type overlay functions for dealing with disconnected operations and aiming at opportunistic transmission [4]. This is shown in the Haggle Project [22], where agents exchange messages with nearby devices. Each agent carries a message until it is close to another device, constructing a global (although delayed) mesh network.

Delayed-state filtering emerges from simultaneous localization and mapping domain to cope with time latencies in landmark initialization and communication. Reference [23] introduced the concept of delayed-state decentralized data fusion, with past estimates retained in the state-space vector for managing historical dependencies. Approaches based on the delayed-state concept differ from the conventional cooperative localization by maintaining a history of agents states to allow fusion of the past data when received. Delayed-state information filter is adopted in [24] and [25], with a canonical-form representation of Gaussian states kept in its sparse information matrix. These studies demonstrated the advantages of the additivity property of the information filter in the update stage and the ability to cope with information loss due to network latencies. However, these approaches require Gaussian assumptions to be satisfied and are not suitable in the case concerned in this paper due to the non-Gaussian properties of the speed and timing profiles for vehicle motion.

III. Long-Term Vehicle Motion Prediction

This section focuses on consistent long-term vehicle motion prediction based on a model of the vehicle that incorporates parameters from the environment and the vehicle history.

A. Modeling Environment Properties

One of the fundamental requirements to improve the prediction of vehicle motion is to obtain an accurate description of the areas of operation. A very large environment can be represented by a road network based on context areas (loading areas, parking lots, etc.) connected by winding road segments and intersections formed by road junctions. As an example, Fig. 1 illustrates this map representation for an actual mining operation. This kind of information is built based on [26] and [27] and is incorporated as prior knowledge.

1) Modeling Road Segments: The most basic model for vehicle motion is to assume a constant velocity. In practice, the speed of a vehicle may vary depending on road conditions, gradients, terrain variations, etc. In addition to the physical constraints, a vehicle will always have a certain probability to stop anywhere and at any time due to operational reasons (taking a break), engine problems, queueing/traffic, or in the event of an accident. Determining the range of potential vehicle dynamics for each part of the road is essential to improve the long-term position estimate. In order to obtain this specific information, each road segment connecting two intersections or areas can be evenly divided into slots. For each road segment in the road network and each slot on the road segment, histograms of the vehicle acceleration and speed are generated with the historical motion data collected from the vehicles in operation. Furthermore, a timing profile is used to determine the probability of the length of time a vehicle will stop on a particular road based on the empirical evidence. An example is shown in Fig. 3(a) for a road connecting the two intersections with real motion data collected from a working mine.

2) Modeling Intersections and Areas: Vehicle behavior at intersections and other important context areas is less structured, with a more complex range of potential trajectories in comparison with on a road. For this reason, it is not feasible to model the vehicle motion using a speed profile as the motion is primarily determined by other factors such as the movement of nearby vehicles. A timing profile is instead used to empirically determine the probability of the time taken for a vehicle to traverse a context area. For each path in an intersection or an area, a timing profile can be built with the statistical distribution of time taken to cross an intersection or an area. In Fig. 3(b), the timing profile is shown to be different for each path crossing the

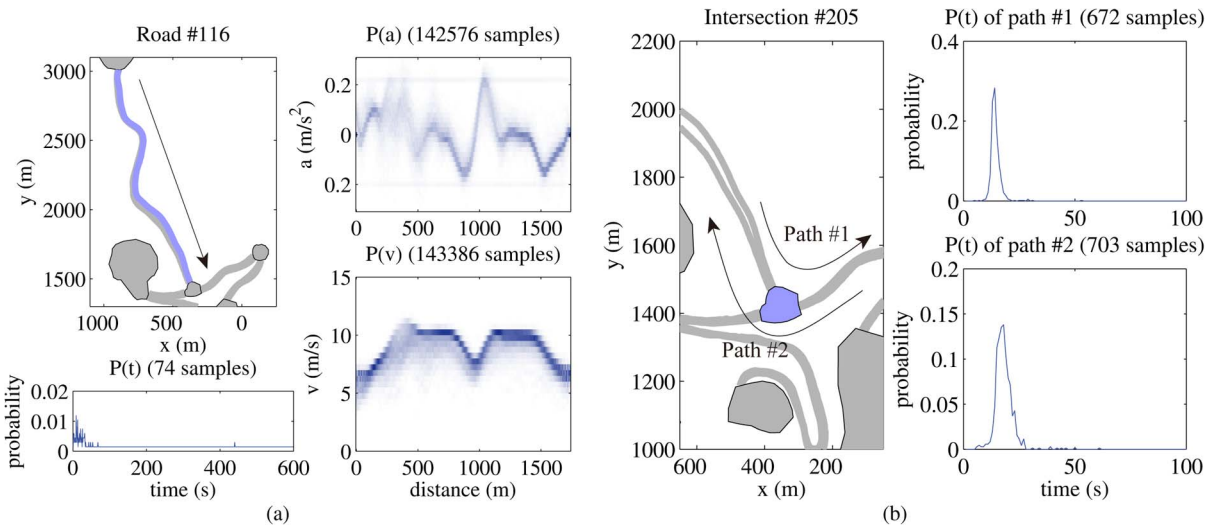

Fig. 3. Acceleration, speed, and timing profiles of road #116 and timing profiles of intersection #205. (a) Variations of acceleration and speed distributions against distance along the road segment in the direction indicated by the arrow. The probability of the length of time a vehicle will stop on the road is determined by the timing profile in (a). (b) Two paths that can be chosen to cross intersection #205. The timing profiles for these two opposite paths are clearly different.

intersection. Unlike a road segment, a path inside an intersection or an area is not geographically divided but treated as a single slot.

3) ASP: The kinematic model for moving vehicles was created using an acceleration–speed profile (ASP) for each position slot on a road segment, statistically representing the range of possible vehicle dynamic characteristics given a particular position. From the kinematic point of view, a strong interrelationship exists between acceleration, speed, and position. Vehicles are likely to speed up on a straight road but slow down when getting close to a corner. A vehicle driving at a slow speed could possibly be decelerating in preparation to stop or preparing to accelerate in order to ramp up to the average speed for that section of the road. The correlation between vehicle acceleration a, speed v, and position $\mathbf{r}$ has been implicitly built into the ASP, which describes $P(a, v|\mathbf{r})$.

B. Multiple-Model Motion Prediction

The prediction and tracking problem stated in this paper can be formulated by multiple-model motion approaches, in which multiple motion models are matched to different motion states of the tracked object. Interested readers may find details and examples on this topic in papers [5], [28]–[30].

A vehicle at time k can be in one of three motion states. These are defined as *moving on roads (MOR)*, *stopping on roads (SOR)*, and *passing intersections and areas (PIA)*, i.e.,

$$S_k \in \{s_1 = \text{MOR}, s_2 = \text{SOR}, s_3 = \text{PIA}\}.$$

A vehicle may stay in the same motion state or move from one state to another. Fig. 4 illustrates the motion state machines and transitions between three states. The state vector for the vehicle at time k is written as

$$\mathbf{x}_k = \begin{bmatrix} \mathbf{r}_k^T & v_k & \tau_k \end{bmatrix}^T$$

where $\mathbf{r}_k \in \mathbb{R}^2$ is the position of the vehicle at time k, $v_k \in \mathbb{R}$ is the instantaneous speed of the vehicle, and τ_k is the time

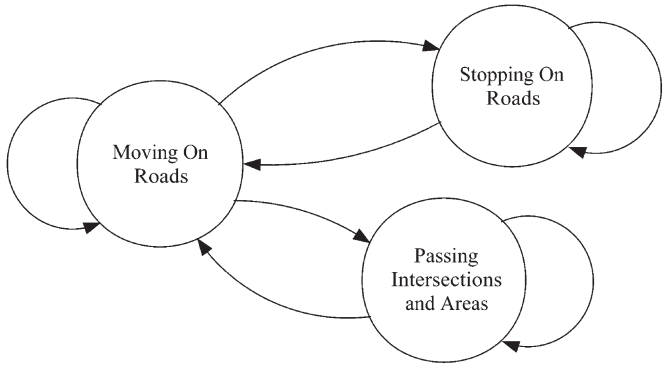

Fig. 4. Motion state machines. A vehicle may stay in a motion state or transit from a state to another when conditions are fulfilled.

remaining for the vehicle to be stopped on a road or to pass through an intersection or an area. τ_k has a positive value for $S_k \in \{s_2, s_3\}$ states, and it is constantly 0 for vehicles in $S_k = s_1$ state.

The transition function represents the probability that a vehicle motion state transits from an initial state s_i to a final state s_j at time k. Thus

$$Ps_{i\to j}(k) \triangleq P(S_k = s_j | S_{k-1} = s_i, \xi_{k-1}) \tag{1}$$

where ξ_{k-1} is an additional condition for the state transition. This condition varies for different pairs of initial and final states. For example, a vehicle has a nonzero probability to transit from *MOR* to *SOR* state when it is moving on a road, and as soon as the stopping time τ_k runs out, the state changes back from *SOR* to *MOR*. Every possible situation for transitions between motion states is considered and dealt with in the transition function presented in (1). For more details on the transition function, please refer to our previous work in [5].

The vehicle dynamics is described by a set of motion models. Each transition of states corresponds to a motion model written as

$$Pm_{i\to j} \triangleq P(\mathbf{x}_k | \mathbf{x}_{k-1}, S_k = s_j, S_{k-1} = s_i). \tag{2}$$

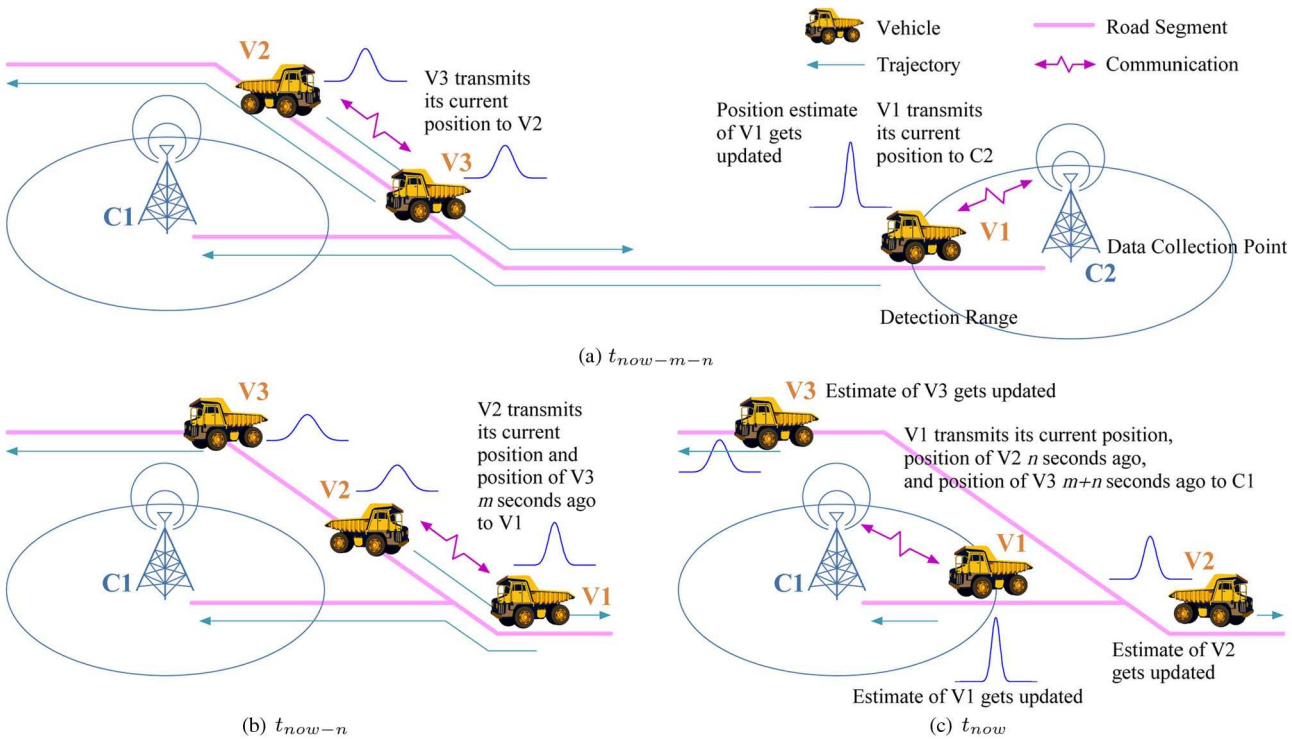

Fig. 5. Benefit of observation harvesting comes from stored V2V interactions between vehicles being brought back to data collection points and used in the filter update stage. In (a), the position information from vehicle V3 was known to V2 from a previous V2V interaction. The information was then forwarded to V1 when V1 and V2 were in communication range, as shown in (b). Lastly, in (c), data collection point C1 receives a delayed update for V2 and V3 through communication with V1, and the position estimates for all three vehicles are evaluated. (a) $t_{\mathrm{now}-m-n}$. (b) $t_{\mathrm{now}-n}$. (c) t_{now}.

The prediction stage of the multiple-model motion tracking for vehicle v_p is written as

$$P\left(\mathbf{x}_k^{v_p}, S_k^{v_p} | \mathbf{Z}_{1:k-1}^{v_p}\right) = \sum_{i=1}^{3}\sum_{j=1}^{3} \int Pm_{i\to j} Ps_{i\to j}(k) P\left(\mathbf{x}_{k-1}^{v_p}, S_{k-1}^{v_p} | \mathbf{Z}_{1:k-1}^{v_p}\right) d\mathbf{x}_{k-1}^{v_p} \tag{3}$$

where $\mathbf{Z}_{1:k-1}^{v_p}$ is an observation vector holding all available observations (e.g., position measurements) with regard to vehicle v_p up to time $k-1$.

So far, the estimation of the vehicle position relies only on the motion prediction. In the following sections, we will propose the observation harvesting mechanism to collect observations and use these to update estimates of vehicles' states.

IV. Observation Harvesting

Observation harvesting refers to the mechanism in which vehicles returning to the communication range of fixed infrastructure (data collection points) provide delayed observations of other vehicles that were encountered during a trip. The centralized base station will update the estimates of vehicle position using direct observations from the vehicles that are currently in communication range (V2I), as well as the egocentric observations collected from interactions between vehicles (V2V) in other areas of the site that do not have direct communication with the base station. The observation harvesting mechanism involves the collection of the second-hand (or third, fourth, etc.) information through V2V communication.

A typical vehicle tracking example demonstrating the observation harvesting process is depicted in Fig. 5: Three vehicles

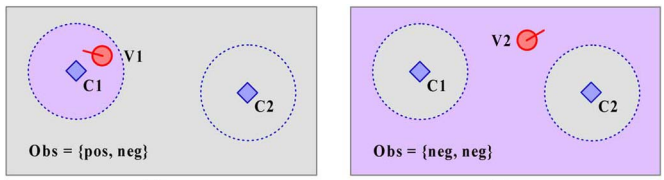

Fig. 6. Positive and negative information scenarios with fixed data collection points C1 and C2. (a) Positive information. Vehicle V1 is detected near collector C1. The location of V1 is constrained to the coverage area of C1, excluding the possibility that V1 is outside the area of C1. (b) Negative information. V2 is outside the coverage area of both C1 and C2, reducing the probability that V2 is close to collectors C1 and C2.

V1, V2, and V3 equipped with GPS are moving in an area with two fixed data collection points C1 and C2. The base station (not shown in the figure) tracks these vehicles with information acquired from each fixed data collection point, which has a limited communication range to adjacent vehicles. Vehicles close to C1 or C2 can be accurately tracked with direct communication of the vehicle state information. Position estimation for vehicles in between these areas relies on the long-term motion model. The mechanism of observation harvesting allows interactions between vehicles to be carried back to the fixed data collectors and used as updates to the position filter.

With observation harvesting, a direct connection between a vehicle and a fixed data collection point is not required to update the position estimate. Each vehicle that returns to a fixed data collector acts as an information carrier for the vehicles that do not return. In addition, when a vehicle is not detected by a data collection point, it is considered negative information. This assists in constraining the possible vehicle location in the absence of new observations.

A. From Information to Observations

Information collected from vehicles in the field is classified according to the information source, usage, method of transmission, and reception. We define the following information categories.

1) Vehicle egocentric observations

Egocentric observations for the absolute egocentric position of each vehicle are obtained from an onboard GPS sensor. This state is dependent only on the vehicle itself. Conventionally, the likelihood function of an absolute egocentric GPS observation for vehicle v_p is mathematically represented by

$$P\left(\mathbf{z}_t^{v_p}|\mathbf{x}_t^{v_p}\right).$$

These observations are broadcast between vehicles using V2V communication, which are stored and forwarded to other vehicles and data collection points using the observation harvesting method described in this paper.

2) Data collection point observations

A data collection point has a known fixed absolute referenced position. The relative information whether a vehicle is nearby can be converted into an absolute referenced observation since the communication range and the location of the collection point are deterministic. When a vehicle establishes V2I communication with a data collection point, it is considered a positive detection, which indicates the presence of the vehicle within the detection area of the collection point. The detection area around the data collection point where V2I communication is possible is bounded and represented by a circle centered at the collection point covering the potential communication range.

On the other hand, if the data collector does not communicate with a vehicle for a period of time, it is considered negative absolute referenced information. The inference from this is that the vehicle is likely to be somewhere outside the detection area. It is important to note that this allows some level of localization if the base station does not have available GPS information for the vehicle. There are two examples demonstrated in Fig. 6, one showing positive information and the other negative.

Provided with an absolute referenced observation from a data collection point c_q located at (x_{c_q}, y_{c_q}), the likelihood function for the position of a vehicle v_p relative to the data collection point is represented by

$$P\left(z_t^{v_p \to c_q}|\mathbf{x}_t^{v_p}, \mathbf{r}^{c_q} = [x_{c_q} \quad y_{c_q}]^T\right).$$

3) Real-time and time-delayed observations

The absolute referenced observations from the infrastructure (i.e., data collection points) are considered real-time information, which becomes available to the base station as soon as it is generated. This includes positive (vehicle is detected) or negative (vehicle not detected) information about the likelihood of a vehicle being in the area around the data collection points.

The egocentric position observations broadcast using V2V communication are shared between vehicles and eventually flow to a data collection point. The relaying of the position observations is defined in this paper as observation harvesting, which is the process where vehicles that are not in contact with the infrastructure can still have position updates transmitted back to the central base station. There is potential for the harvested observations to have significant time delay (potentially on the order of minutes for large environments); thus, the localization filter at the base station must consider both real-time and delayed observations.

There is a special case where a vehicle egocentric position observation is considered real-time information. When a vehicle is within the communication range of any data collection point, its egocentric observations are immediately known by the base station through V2I communication. This is the best case in the observation harvesting process as the time delay is zero.

TABLE I
OBSERVATIONS FROM INFORMATION IN FIG. 5(C)

Information Description at t_{now}	Observation Type
C1 obtains the position of V1 through direct communication	real-time[1]
C1 acquires from V1 the position of V3 $m+n$ seconds ago	time delayed
C1 detects V1 within communication range	real-time, positive
C2 does not detect V1, V2 or V3	real-time, negative

[1] The position of V1 generated directly from the GPS at t_{now} is collected by C1 immediately.

For the illustrative example in Fig. 5(c), information collected by the base station is converted into observations, which can be used to constrain estimates of vehicles' states. Table I shows a summary of some examples.

B. Observation Harvesting Algorithm Overview

The proposed observation harvesting algorithm allows egocentric position updates from vehicles, with some time delays, to be shared and harvested by the base station. The most informative information is kept in every vehicle and synchronized when a pair of vehicles are in communication range. When a vehicle passes a data collection point (fixed infrastructure), observations collected by the vehicle are downloaded and used to track all vehicles. Within the base station, real-time V2I observations generated by data collectors distributed in the field are also used in the tracking process. An overview of the observation harvesting algorithm is shown in Fig. 7.

To summarize, the information conveyed in every vehicle is composed of the following:

1) $\mathbf{B}_k^{v_p}$: local egocentric observation pool, which is augmented over time with new observations based on new sensor information;
2) $\mathbf{L}_k^{v_p}$: most informative observation vector (MIOV), which refers to an aggregation of the most informative observations about the vehicle itself and others. The MIOV information in a vehicle is extracted at every new time step from its local egocentric observation pool, i.e.,

$$\mathbf{L}_k^{v_p} = \left[\left(\mathbf{z}_m^{v_1}\right)^T \quad \cdots \quad \left(\mathbf{z}_m^{v_p}\right)^T \quad \cdots \quad \left(\mathbf{z}_m^{v_N}\right)^T\right]^T$$

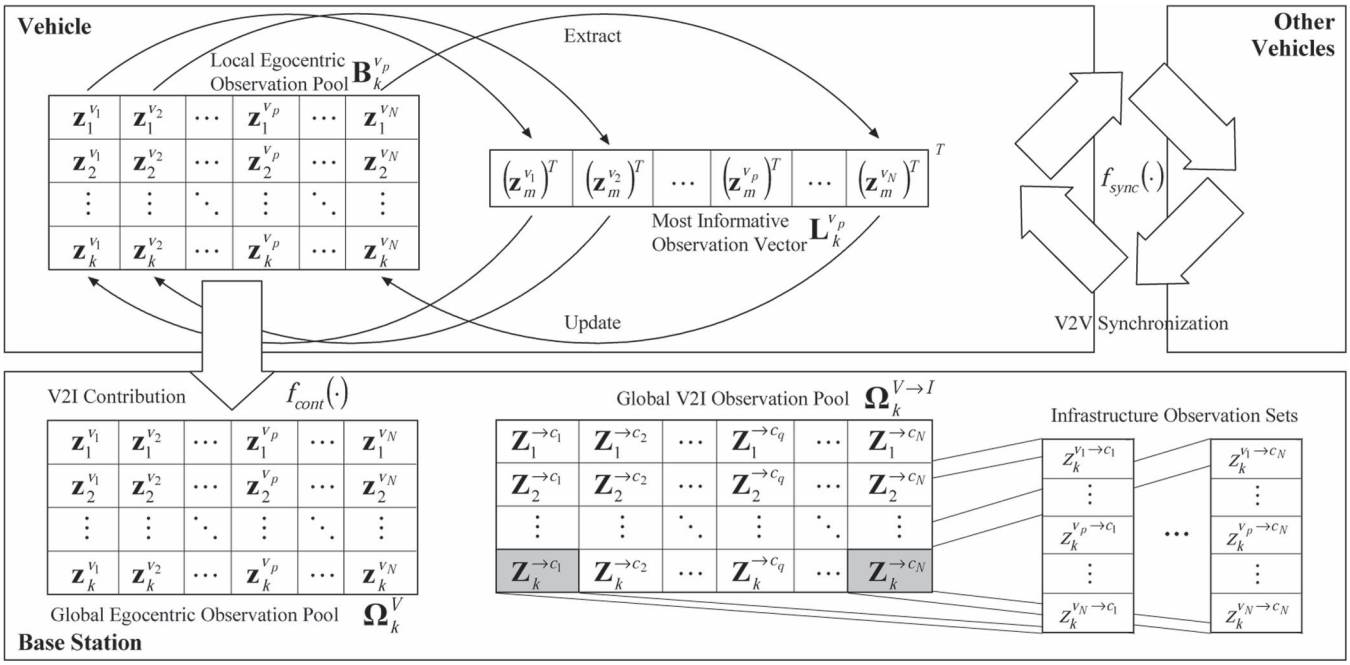

Fig. 7. Overview of the observation harvesting algorithm.

where each element is the most informative observation regarding every vehicle.

The base station keeps the information harvested in the following form:

1) $\mathbf{\Omega}_k^V$: global egocentric observation pool, where egocentric observations collected (harvested) from all N_v vehicles in the field are merged together;
2) $\mathbf{\Omega}_k^{V\to I}$: global V2I observation pool, which keeps real-time observations from all N_c data collectors distributed in the field observing each vehicle.

The proposed observation harvesting algorithm with MIOV is capable of operating in a low-bandwidth P2P network. It provides a simple but effective way to gain the best position knowledge of all vehicles running in the field. To prevent overloading the available communication bandwidth, only the most informative observations are exchanged in a data synchronization process between a pair of vehicles. Among all observation sets with absolute observations available, the most informative observation usually has the time stamp closest to the present time.

C. Synchronization Process

The synchronization process of the MIOV occurs when two vehicles meet. This process involves bidirectional exchange of data between the two vehicles. After this process, the MIOVs in each of the two vehicles are expected to be identical.

Between two vehicles v_p and v_q, the whole synchronization process $f_{\text{sync}}(\cdot)$ is as described in Table II. The process begins with extracting and comparing time profiles of MIOVs (defined as $\mathbf{T}_k^{v_p}$, $\mathbf{T}_k^{v_q}$) of the two nodes. In order to minimize the bandwidth, only the information in the MIOV with a newer time stamp is transferred from one node to the other. This essentially means that each vehicle shares the best information they have about all other vehicles they have been in communication

TABLE II
SYNCHRONIZATION PROCESS

$\mathbf{L}_{k+}^{v_p} = \mathbf{L}_{k+}^{v_q} \leftarrow f_{sync}\left(\mathbf{L}_k^{v_p}, \mathbf{L}_k^{v_q}\right)$

extract $\mathbf{T}_k^{v_p}$ from $\mathbf{L}_k^{v_p}$
extract $\mathbf{T}_k^{v_q}$ from $\mathbf{L}_k^{v_q}$
for $i = 1$ to N_v **do**
  if $T_{k,v_i}^{v_p}$ in $\mathbf{T}_k^{v_p} > T_{k,v_i}^{v_q}$ in $\mathbf{T}_k^{v_q}$ **do**
    replace $\mathbf{z}_m^{v_i}$ in $\mathbf{L}_k^{v_q}$ by $\mathbf{z}_m^{v_i}$ in $\mathbf{L}_k^{v_p}$
  else if $T_{k,v_i}^{v_q}$ in $\mathbf{T}_k^{v_q} > T_{k,v_i}^{v_p}$ in $\mathbf{T}_k^{v_p}$ **do**
    replace $\mathbf{z}_m^{v_i}$ in $\mathbf{L}_k^{v_p}$ by $\mathbf{z}_m^{v_i}$ in $\mathbf{L}_k^{v_q}$
  end if
end for
$\mathbf{L}_{k+}^{v_p} = \mathbf{L}_k^{v_p}$ and $\mathbf{L}_{k+}^{v_q} = \mathbf{L}_k^{v_q}$

with. After the synchronization process, the local egocentric observation pool is updated with the new information received.

The amount of data transferred in the synchronization process is no larger than the size of MIOV, i.e., N_v absolute observations. With only a small amount of data exchanged, the synchronization process provides a simple, short, and effective method to disseminate the most informative information among all vehicles in the field.

D. Updating the Global Observation Pool

We define a contribution process, whereby each vehicle uploads (contributes) observations in the local egocentric observation pool to the base station when in communication with a fixed data collection point. The data transmission in the process is unidirectional. A description on the contribution process $f_{\text{cont}}(\cdot)$ could be found in Table III.

The last contribution time $T_{\text{cont}}^{v_p\to I}$ is kept in each vehicle to minimize the communication bandwidth requirements. When the process occurs between a vehicle v_p and the base station, only the information in the local egocentric observation pool of vehicle v_p with a time stamp later than the last contribution

TABLE III
CONTRIBUTION PROCESS

$\mathbf{\Omega}_{k+}^{V}, T_{cont}^{v_p \to I} \leftarrow f_{cont}\left(\mathbf{\Omega}_{k}^{V}, \mathbf{B}_{k}^{v_p}, T_{cont}^{v_p \to I}\right)$

for $t = T_{cont}^{v_p \to I} + 1$ to k **do**
  for $i = 1$ to N_v **do**
    vehicle v_p transmits $\mathbf{z}_t^{v_i}$ in $\mathbf{B}_k^{v_p}$ to $\mathbf{\Omega}_k^V$
  end for
end for
$T_{cont}^{v_p \to I} = k$
$\mathbf{\Omega}_{k+}^{V} = \mathbf{\Omega}_{k}^{V}$

TABLE IV
MAXIMUM AND MEAN BANDWIDTH COSTS ON P2P COMMUNICATION

	Quantity of Obs. Transmitted/Received	
	Maximum	Mean
V2V	$N_v - 1$	$N_v/2$
V2I	$N_v \tau^{v_p \to I}$	$\bar{\tau}^{v_p \to I} + (N_v - 1)\,\eta$

time $T_{\text{cont}}^{v_p \to I}$ is transferred to the global egocentric observation pool. After the contribution process, the last contribution time is updated to the present time.

E. Cost Analysis of Communication Bandwidth

Define

1) $\bar{\tau}^{V \to V}$ as the average communication time interval between vehicles;
2) $\tau^{v_p \to I}$ and $\bar{\tau}^{v_p \to I}$ as the communication time interval between a vehicle v_p and the infrastructure and its average value, respectively;
3) interval ratio $\eta = \bar{\tau}^{v_p \to I} / \bar{\tau}^{V \to V}$, which means that, on average, the vehicle v_p meets another particular vehicle η times during the time interval $\bar{\tau}^{v_p \to I}$.

Regardless of the communication intervals, the maximum intervehicle communication bandwidth is constant with a value of $N_v - 1$ absolute observations. Table IV also suggests that the maximum V2I bandwidth is proportional to the time elapsed since the last contribution time. Increasing either the quantity of data collection points or the communication range would reduce the V2I communication interval and the requirements for V2I communication bandwidth. Alternatively, optimization on the bandwidth cost could be achieved by introducing a sliding time window into the filter, which is elaborated in Section V-E.

V. TRACKING WITH DELAYED OBSERVATIONS

A. V2I Proximity Detection

As detailed before, we assume that one or more data collection points are distributed in the field to operate as observers. In this paper, V2I observations come from proximity detection between vehicles and the data collection points. Specifically, the wireless transceiver mounted at a fixed data collection point provides a binary connectivity observation when a vehicle is able to either communicate with it or not. As the signal coverage range of a wireless transceiver is limited up to only a few hundred meters, this paper considers both positive and negative information from the data collection points, as also described in [31] and [32].

TABLE V
LIKELIHOODS FROM INFORMATION IN FIG. 5(C)

	Observer (at $t = t_{now}$)				
Target	V1	V2	V3	C1	C2
V1	$\widetilde{\Psi}_t^{V1}$	N/A	N/A	$\Psi_t^{V1 \to C1}$	$\Psi_t^{V1 \to C2}$
V2	N/A	$\widetilde{\Psi}_t^{V2}$	N/A	$\Psi_t^{V2 \to C1}$	$\Psi_t^{V2 \to C2}$
V3	N/A	N/A	$\widetilde{\Psi}_t^{V3}$	$\Psi_t^{V3 \to C1}$	$\Psi_t^{V3 \to C2}$

A probabilistic approach is adopted with a purpose of modeling realistic V2I proximity detection given connectivity measurements. Connectivity is a binary quantization of received signal strength intensity measurement [33], without considering signal propagation models. The measurement could be either *positive connectivity* (*PC*) or *negative connectivity* (*NC*), where *NC* of two nodes is considered a piece of negative information.

Provided that the position of a data collector c_q is a Dirac delta function at (x_{c_q}, y_{c_q}), the likelihood function given an absolute referenced connectivity observation between a vehicle v_p and the data collector at time t is represented by

$$\Psi_t^{v_p \to c_q} \triangleq P\left(z_t^{v_p \to c_q} | \mathbf{x}^{v_p}, \mathbf{r}^{c_q} = [x_{c_q} \quad y_{c_q}]^T\right) \tag{4}$$

where $z_t^{v_p \to c_q} \in [\text{PC}, \text{NC}]$ is a V2I connectivity observation. A *PC* event is observed when the data collection point receives a packet from vehicle v_p; otherwise, an *NC* event occurs. Fig. 6 gives examples of the binary connectivity observation.

B. Egocentric Observations From Vehicles

The likelihood function for an absolute (GPS-based) egocentric observation of vehicle v_p at time t is denoted by

$$\widetilde{\Psi}_t^{v_p} \triangleq P\left(\mathbf{z}_t^{v_p} | \mathbf{x}_t^{v_p}\right). \tag{5}$$

Although an absolute egocentric observation could be either real time (as in Table I) or time delayed, the likelihood functions are considered the same for convenience. A real-time observation is considered as a special case of the time-delayed observation with zero delay.

Continuing the example shown in Fig. 5(c), Table V interprets observations gathered by the base station at time t_{now} in the form of likelihood functions defined in (4) and (5).

Note that although vehicles communicate with each other, V2V relative position measurements are not yet considered in the fusion stage. This is because it requires the consideration of cross correlations between vehicles.

C. Bayesian Estimation

Traditional approaches based on sequential Bayesian estimation only consider observations conditional on the present state. They are, therefore, of low performance in tracking problems with delayed observations. Instead, the filtering algorithm adopted in this paper maintains the full history of vehicle states. With historical states maintained in the filter, information from delayed observations is able to be fused.

We make the following definitions.

1) Define $\mathbf{\Omega}_{k|k-1}^{v_p \to I}$ as a set of new real-time V2I observations from the infrastructure at time k.

2) $\mathbf{\Omega}_{k|k-1}^{v_p}$ is defined to be a collection of the delayed egocentric observations of vehicle v_p most recently received by the base station at time k.

Information contained in these two observation sets will be fused into the filter in its update stage. They are obtained by relative complement operations of global observation pools at two successive time steps. Respectively, we have

$$\begin{aligned}\mathbf{\Omega}_{k|k-1}^{v_p\to I} &= \mathbf{\Omega}_{k}^{v_p\to I} \setminus \mathbf{\Omega}_{k-1}^{v_p\to I} \\ &= \left[z_k^{v_p\to c_1} \quad \cdots \quad z_k^{v_p\to c_q} \quad \cdots \quad z_k^{v_p\to c_N}\right]^T \\ \mathbf{\Omega}_{k|k-1}^{v_p} &= \mathbf{\Omega}_{k}^{v_p} \setminus \mathbf{\Omega}_{k-1}^{v_p}\end{aligned}$$

where $\mathbf{\Omega}_{k}^{v_p\to I}$ holds all relative vehicle v_p to infrastructure observations up to time k in the global V2I observation pool $\mathbf{\Omega}_{k}^{V\to I}$, whereas $\mathbf{\Omega}_{k}^{v_p}$ keeps every egocentric observation of v_p up to time k, which are stored in the global egocentric observation pool $\mathbf{\Omega}_{k}^{V}$. Note that $\mathbf{\Omega}_{k|k-1}^{v_p}$ could be empty.

To track vehicles with delayed egocentric observations, the filter keeps full historical state information for each vehicle. At time k, the full states of vehicle v_p are represented as

$$P\left(\mathbf{x}_{0:k}^{v_p}, S_{0:k}^{v_p} | \mathbf{\Omega}_{k}^{v_p\to I}, \mathbf{\Omega}_{k}^{v_p}\right).$$

The prediction stage presented in (3) and the update/fusion stage can be combined together to yield

$$\begin{aligned}&P\left(\mathbf{x}_{0:k}^{v_p}, S_{0:k}^{v_p} | \mathbf{\Omega}_{k}^{v_p\to I}, \mathbf{\Omega}_{k}^{v_p}\right) \\ &\quad\propto \left(\prod_{q=1}^{N_c} \Psi_k^{v_p\to c_q}\right)\left(\prod_{\mathbf{z}_t^{v_p}\in\mathbf{\Omega}_{k|k-1}^{v_p}} \widetilde{\Psi}_t^{v_p}\right) \\ &\qquad\times \sum_{i=1}^{3}\sum_{j=1}^{3}\int Pm_{i\to j} Ps_{i\to j}(k) \\ &\qquad\times P\left(\mathbf{x}_{0:k-1}^{v_p}, S_{0:k-1}^{v_p} | \mathbf{\Omega}_{k-1}^{v_p\to I}, \mathbf{\Omega}_{k-1}^{v_p}\right). \qquad (6)\end{aligned}$$

D. Particle Filtering Algorithm

Gaussian-based tracking algorithms are not appropriate due to non-Gaussian properties of the speed and timing profiles in the vehicle motion model. In addition, the vehicle prediction/tracking problem presents nonlinearities in motion state transitions and dynamics models. For this reason, particle filtering is well suited for the type of problem discussed in this paper. So far, it has been widely used in vision-based traffic features recognition/detection approaches to track vehicles [34], pedestrians [35], lanes [36], or traffic signs [37].

In the proposed algorithm, each vehicle running in the field is tracked by a separate particle filter maintained on a central base station, which uses $k+1$ sets of particles to keep track of the complete history states of the vehicle up to time k.

Define a particle base keeping $k+1$ collections of particles, which correspond to $k+1$ states of the vehicle v_p, i.e.,

$$\Theta_k^{v_p} = \begin{bmatrix} \left\{\mathbf{x}_0^i, S_0^i, w_0^i\right\}_{i=1}^{L} \sim P\left(\mathbf{x}_0^{v_p}, S_0^{v_p}\right) \\ \left\{\mathbf{x}_1^i, S_1^i, w_1^i\right\}_{i=1}^{L} \sim P\left(\mathbf{x}_1^{v_p}, S_1^{v_p} | \mathbf{\Omega}_1^{v_p\to I}, \mathbf{\Omega}_1^{v_p}\right) \\ \vdots \\ \left\{\mathbf{x}_k^i, S_k^i, w_k^i\right\}_{i=1}^{L} \sim P\left(\mathbf{x}_k^{v_p}, S_k^{v_p} | \mathbf{\Omega}_k^{v_p\to I}, \mathbf{\Omega}_k^{v_p}\right) \end{bmatrix}$$

TABLE VI
PARTICLE FILTERING WITH DELAYED OBSERVATIONS

$\Theta_k^{v_p} \leftarrow$ *Particle_filter* $\left(\Theta_{k-1}^{v_p}, \mathbf{\Omega}_{k-1}^{v_p}, \mathbf{\Omega}_{k}^{v_p}, \mathbf{\Omega}_{k}^{v_p\to I}\right)$

calculate $\mathbf{\Omega}_{k|k-1}^{v_p} = \mathbf{\Omega}_{k}^{v_p} \setminus \mathbf{\Omega}_{k-1}^{v_p}$
if $\mathbf{\Omega}_{k|k-1}^{v_p}$ is not empty **do**
  $T_s = f_{min}\left(\mathbf{\Omega}_{k|k-1}^{v_p}\right)$
else do
  $T_s = k$
end if
load particles $\{\mathbf{x}_{T_s-1}^i, S_{T_s-1}^i, w_{T_s-1}^i\}_{i=1}^{L}$ from $\Theta_{k-1}^{v_p}$
for $t = T_s$ to k **do**
  for $i = 1$ to L **do**
    propagation: draw $S_t^i \sim P\left(S_t | S_{t-1}^i, \xi_{t-1}^i\right)$
    draw $\mathbf{x}_t^i \sim P\left(\mathbf{x}_t | \mathbf{x}_{t-1}^i, S_t^i, S_{t-1}^i\right)$
    update weight with V2I observations:
    $w_t^i = \left(\prod_{q=1}^{N_c} \Psi_t^{v_p\to c_q}\right) w_{t-1}^i$
    update weight with egocentric observation:
    $w_t^i = \widetilde{\Psi}_t^{v_p} w_t^i$ if $\widetilde{\Psi}_t^{v_p}$ exists
  end for
  normalize weights $\{w_t^i\}_{i=1}^{L}$
  if $\hat{N}_{eff} < N_{thr}$ **do**
    resample with replacement L particles from $\{\mathbf{x}_t^i, S_t^i, w_t^i\}_{i=1}^{L}$ according to $\{w_t^i\}_{i=1}^{L}$
  end if
  replace $\{\mathbf{x}_t^i, S_t^i, w_t^i\}_{i=1}^{L}$ in $\Theta_{k-1}^{v_p}$ if $t < k$
end for
$\Theta_k^{v_p} \leftarrow \begin{bmatrix} \Theta_{k-1}^{v_p} \\ \{\mathbf{x}_k^i, S_k^i, w_k^i\}_{i=1}^{L} \end{bmatrix}$

where $\mathbf{x}_k^i$ is further factorized to $\mathbf{x}_k^i = \left[(\mathbf{r}_k^i)^T \quad v_k^i \quad \tau_k^i\right]^T$.

Information in both the global V2I observation pool and the global egocentric observation pool is fused in the filter in a nonsynchronous mode. Without the availability of egocentric observations received from vehicles, the filtering continues with prediction and updates with real-time V2I measurements from fixed data collection points. The filtering is then restarted from a historical state on arrival of delayed observations. The earliest time stamp T_s in the new received egocentric observations $\mathbf{\Omega}_{k|k-1}^{v_p}$ at time k determines the time from which the particle filter restarts.

The particle filtering algorithm is initialized by drawing L particles to represent the initial state

$$\Theta_0^{v_p} = \left[\left\{\mathbf{x}_0^i, S_0^i, w_0^i\right\}_{i=1}^{L} \sim P\left(\mathbf{x}_0^{v_p}, S_0^{v_p}\right)\right].$$

The algorithm for each vehicle is presented in Table VI in the form of a pseudocode. To prevent weight degeneracy, resampling is adopted in the algorithm when the effective particles quantity $\hat{N}_{\text{eff}}$ is below a threshold N_{thr}.

E. Computational Complexity and Optimization

The proposed particle filter is of higher computational cost than conventional sequential approaches, which have a time complexity of $O(L)$ for each vehicle in each iteration. We have found that the motion prediction step in the proposed approach is the major contributor of the computational burden as it deals with complicated transitions of vehicle states and multiple vehicle models. Consequently, the computational complexity mainly depends on the number of steps the filter rewinds back during an iteration. In the worst case, the proposed particle filter restarts from the last contribution time $T_{\text{cont}}^{v_p\to I}$. Thus, the

Fig. 8. Haul trucks running in a mining field.

restart point T_s, as shown in Table VI, could be a value between $k - \tau^{v_p \to I} + 1$ and the present time k, which means that the time complexity of the proposed particle filter is no more than $O(\tau^{v_p \to I} L)$ for a vehicle v_p. $\tau^{v_p \to I}$ was previously defined as the time elapsed since the last contribution time of the vehicle. The actual time complexity varies depending on the V2V and V2I communication activities in the field (see Section VI-D for detailed discussions).

The algorithm can be optimized by introducing a time sliding window with which only historical states within T_w seconds before the present time k are kept. With T_s then constrained by $[k - T_w + 1, k]$, the maximum time complexity in an iteration is reduced to $O(\tau_m L)$, where $\tau_m = \min(\tau^{v_p \to I}, T_w)$. Therefore, by setting the maximum allowable time delay for vehicle observations in the use of the time sliding window, the computational cost of rerunning the filter is bounded. As observations with delay time larger than the time window T_w would be discarded, the choice of the time window length is essentially a tradeoff between estimation accuracy and computational cost.

The communication bandwidth cost between vehicles and infrastructure will also be bounded by introducing the time sliding window, as observations out of the window are not transmitted. Consequently, the maximum amount of observations transmitted or received in a single V2I transaction will be reduced to $N_v \tau_m$.

VI. Experimental Validation

A. Experiment Setup

Real data from a working mine operation (see Fig. 8) were used to demonstrate the vehicle tracking algorithm presented. The vehicle state information collected includes vehicle positions and speeds taken from GPS sensors. Postprocessing was performed to evaluate stopping probability on roads, time taken to resume running, and the length of time a vehicle spent on an area or an intersection. The acceleration, speed, and timing profiles are evaluated for each road segment, intersection, and area based on historical data of 25 days (600 h) collected from five vehicles. During the experiment, the wireless transceiver mounted on each vehicle was enabled so that the vehicles could communicate when in proximity.

B. Entropy of Target Agent(s)

Entropy is adopted as a metric to measure the performance of the estimation algorithm. As an indicator of the uncertainty contained in position estimates of the target vehicle, the entropy for a single mobile agent at time k is calculated by

$$H(\mathbf{x}_k) = -\sum_{s=1}^{n} \mathrm{pm}_k(s) \log_2 \mathrm{pm}_k(s)$$

where $\mathrm{pm}_k(s)$ is the probability mass of position slot s from total n slots along the vehicle's route at time k. A path inside an area/intersection is considered as an individual position slot.

The probability mass on position slot s could be calculated by summing up all weights of particles on the slot, i.e.,

$$\mathrm{pm}_k(s) = \sum_{\mathbf{r}_k^i \in s} w_k^i.$$

When analyzing multiple agents cases (for example, N_v vehicles), fleet entropy is used by adding up the entropy of each agent in the fleet. A brief description of the fleet entropy could also be found in [20]. Thus

$$H(\mathbf{X}_k) = \sum_{p=1}^{N_v} H\left(\mathbf{x}_k^{v_p}\right)$$

where $\mathbf{X}_k = [(\mathbf{x}_k^{v_1})^T \quad \cdots \quad (\mathbf{x}_k^{v_p})^T \quad \cdots \quad (\mathbf{x}_k^{v_N})^T]^T$.

C. Experimental Results

Although the algorithm was run with a number of vehicles, we use a subset to show the results in a more clear manner. In this case, we selected three vehicles (V1, V2, and V3) that were moving in the area of operation with two fixed data collection points (C1 and C2) installed [see Fig. 10(a) for the detailed layout and routes on the field map]. The road map is automatically generated and continuously updated using raw GPS data that are collected as part of the everyday operation of the vehicles in the field. The approach for automated map building is described in [27] and in earlier work, namely, [26] and [38]. According to Fig. 9, which depicts the relative distance and interactions between two vehicles, events at some important time points are summarized in chronological order as follows:

- $T_{\mathrm{V1}\to\mathrm{C1}}$: the last communication time between V1 and C1;
- $T_{\mathrm{V2}\to\mathrm{C2}}$: the last communication time between V2 and C2;
- $T_{\mathrm{V1}\to\mathrm{V3}}$: the last time V3 observed V1;
- $T_{\mathrm{V3}\to\mathrm{V1}}$: the last time V1 observed V3;
- $T_{\mathrm{V3}\to\mathrm{C1}}$: the first communication time between V3 and C1;
- $T_{\mathrm{V1}\to\mathrm{V2}}$: the last time V2 observed V1;
- $T_{\mathrm{V2}\to\mathrm{V1}}$: the last time V1 observed V2;
- $T_{\mathrm{V1}\to\mathrm{C2}}$: the first communication time between V1 and C2.

To describe the sequence of events, V1 left the communication range of C1 at time $T_{\mathrm{V1}\to\mathrm{C1}}$ and drove south, whereas V2 left C2 at time $T_{\mathrm{V2}\to\mathrm{C2}}$ and drove north. V1 passed V3 followed by V2 during this trip. V3 drove to C1 at time $T_{\mathrm{V3}\to\mathrm{C1}}$, after having passed V1 and collected its most informative position information up to time $T_{\mathrm{V1}\to\mathrm{V3}}$ through V2V synchronization.

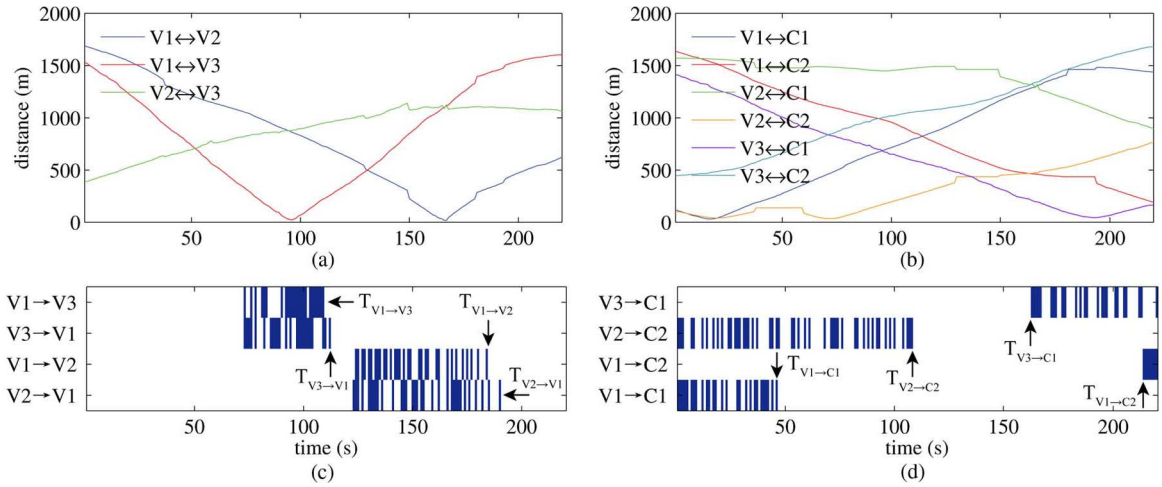

Fig. 9. Interactions in V2V and V2I. (a) and (b) Change in relative distance in each of three vehicles pairs (V2V) with time and between vehicles and data collection points (V2I), respectively. Troughs in distance lines represent physical proximity points of two nodes. In (c) and (d), which plot V2V and V2I communication activities, respectively, blue denotes that the successful communication between nodes was achieved and blank otherwise. More specifically, $T_{\mathrm{V3}\rightarrow\mathrm{V1}} = 111$ s, $T_{\mathrm{V1}\rightarrow\mathrm{V3}} = 108$ s, $T_{\mathrm{V1}\rightarrow\mathrm{V2}} = 183$ s, and $T_{\mathrm{V2}\rightarrow\mathrm{V1}} = 189$ s in (c). For V2I communication in (d), $T_{\mathrm{V1}\rightarrow\mathrm{C1}} = 45$ s and $T_{\mathrm{V2}\rightarrow\mathrm{C2}} = 107$ s, whereas $T_{\mathrm{V3}\rightarrow\mathrm{C1}} = 162$ s and $T_{\mathrm{V1}\rightarrow\mathrm{C2}} = 213$ s.

The data collector C1 captured the time-delayed position update from V3, and the base station used this to improve the estimate of the position of V1. This is illustrated in Fig. 10(c) at the time marked $T_{\mathrm{V3}\rightarrow\mathrm{C1}}$.

Similarly, V1 provided the base station with its egocentric observations and a position update for V2 after arriving at C2 at time $T_{\mathrm{V1}\rightarrow\mathrm{C2}}$. The position information from V2 that was harvested by V1 resulted in an improvement in the position estimate of V2, as illustrated in Fig. 10(f), at the time marked $T_{\mathrm{V1}\rightarrow\mathrm{C2}}$.

Tracking results without V2V communication enabled are shown for comparison in Fig. 10(b) and (e). These figures demonstrate the significant benefits of introducing intervehicle communication and the associated observation harvesting mechanism presented in this paper. The position tracking of V3 does not show any difference with V2V enabled or disabled. This is because V3 provides a direct position update to the base station before any of the other vehicles. Without observation harvesting (V2V disabled), the results are the same as in our previous work [5].

In terms of estimation errors and entropies, Fig. 11 compares the tracking performance with V2V disabled and enabled, clearly illustrating the improvements with the incorporation of V2V communication. The tracking with V2V communication enabled is represented with blue lines. It can be seen that after some time, it outperforms the tracking with V2V disabled (denoted by green lines). This is true in both individual and fleet estimation errors and entropies.

D. Discussion

The motion prediction model proposed in this paper provides an accurate and consistent long-term prediction of vehicle positions in the absence of observations. The road model was built from the data collected from five vehicles in operation on site, resulting in 25 days worth of data. We found that there was no significant difference to the results when the road model was generated using only half of the available vehicle data (approximately two weeks). Based on this, it appears that the model generalizes well to new instances of vehicle movements, as the models for each separate half of the data were very similar.

The accuracy of the GPS obtained position information can be degraded in certain conditions due to signal interference, multipath, poor satellite configuration, and so forth. The tracking accuracy from the base station position estimates, however, is not heavily influenced by this as the position uncertainty of each vehicle is generally an order of magnitude higher than the GPS error after several minutes with no updates. Fig. 10 shows how the position uncertainty of each vehicle grows to the order of hundreds of meters in minutes when the base station is not provided with new position information. This indicates that the potential GPS error (on the order of 10 m) is not significant to the overall tracking performance.

Negative information contributes to improve the estimation performance in the absence of available positive observations. Vehicles that are not in direct communication with data collectors are able to be tracked with delayed observations brought back by returning vehicles.

Since information becomes less useful (or "diluted") as time goes on, tracking accuracy could be improved by reducing the delays in observations. This can be achieved by shortening the "*blind time*," i.e., the average time interval between the base station receiving observations about the same vehicles. The approaches can include the following:

- increasing quantity/density of data collection points: to shorten the time taken for a vehicle to move from a data collection point to another;
- optimizing layout of data collection points: they are recommended to be placed at regions with heavy traffic and high timing uncertainty, such as special context areas and intersections, so that vehicles are detected by the data collectors more of the time.

For example, for a duration of almost 1 min in the experiment, i.e., between time points $T_{\mathrm{V2}\rightarrow\mathrm{C2}}$ (107 s) and $T_{\mathrm{V3}\rightarrow\mathrm{C1}}$

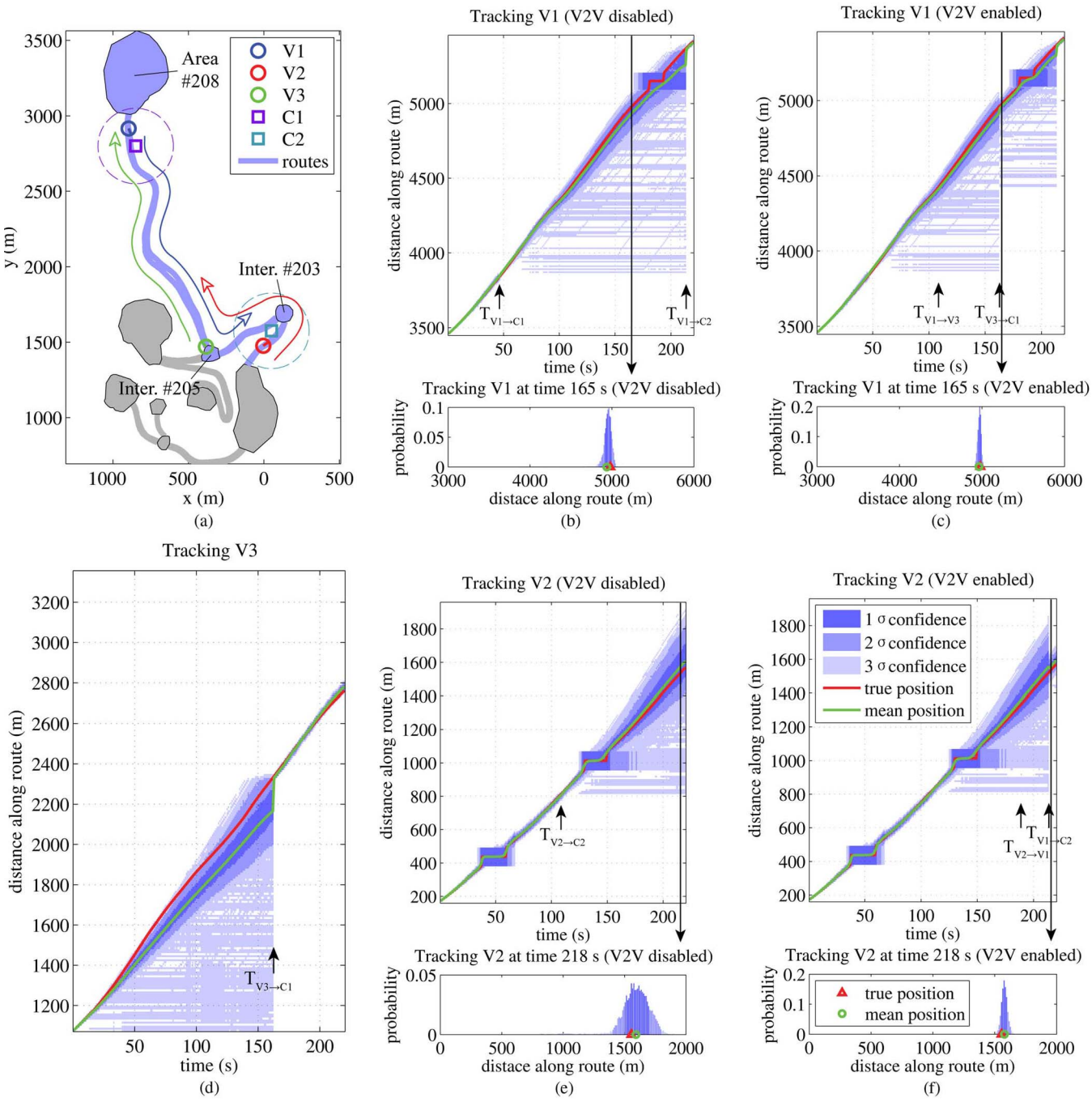

Fig. 10. Tracking results of the multiple vehicles scenario. In (a), three vehicles were running in a field with two data collection points installed near intersection #203 and area #208. Each data collection point established a signal circle with a radius of 250 m. (a) also shows the vehicle routes on the map. The vehicles were operating between intersections #203 and #205 and area #208. V1 began a trip on the road near area #208, V2 began on a road adjacent to intersection #203, and V3 began near intersection #205. (b) and (c) show the tracking of V1 with V2V disabled and enabled, respectively. (c) demonstrates a more accurate position estimate of V1 from time $T_{\mathrm{V3}\rightarrow\mathrm{C1}}$ (162 s) onward after a position update was delivered to the base station by V3. In (f), an improved position estimate for V2 is shown with V2V enabled from time $T_{\mathrm{V1}\rightarrow\mathrm{C2}}$ (213 s) onward in comparison with the tracking results with V2V disabled in (e). This is a result of V1 delivering a position observation from V2 to the base station as a delayed observation. (d) Tracking V3 (same results with V2V enabled and disabled). There were no delayed updates provided for V3, meaning that the results are identical with or without V2V communication.

(162 s), the infrastructure could not detect any of the vehicles, and the position estimation of all three vehicles had to rely on the motion prediction alone. In this case, the *blind time* could be reduced by either deploying additional data collection point(s) somewhere between the two existing ones or relocating C2 near intersection #205, where vehicles generally take more time to traverse.

The *blind time* can also be reduced by the following:

- increasing the density of vehicles: to increase the frequency of V2V communication between vehicles, which consequently increases the sharing of information between vehicles. This will happen naturally in operations with a large number of vehicles, potentially making the proposed

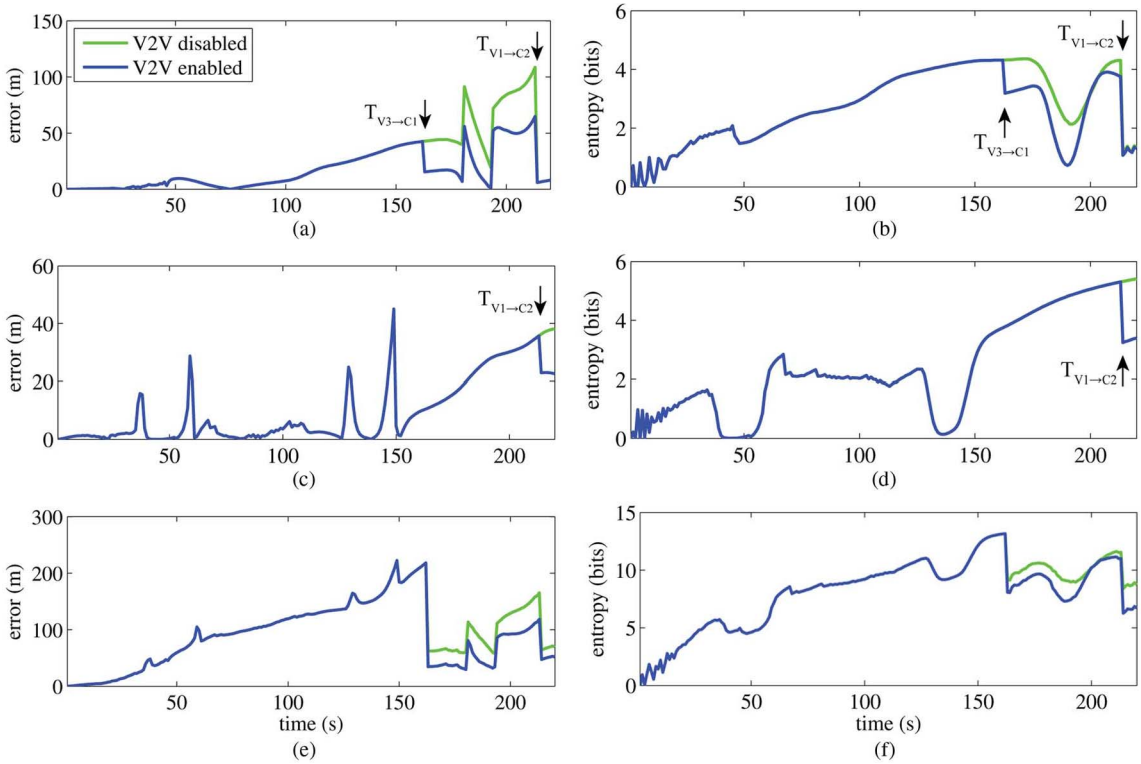

Fig. 11. Comparisons of estimated errors and entropies. Reduction in errors and entropies, respectively, of V1 is shown in (a) and (b) from time $T_{\mathrm{V3}\to\mathrm{C1}}$ on. Likewise, improvements can be seen for V2 after time $T_{\mathrm{V1}\to\mathrm{C2}}$, as illustrated in (c) and (d). (e) and (f) suggest an improvement in total estimation errors and fleet entropies, respectively, with observation harvesting introduced.

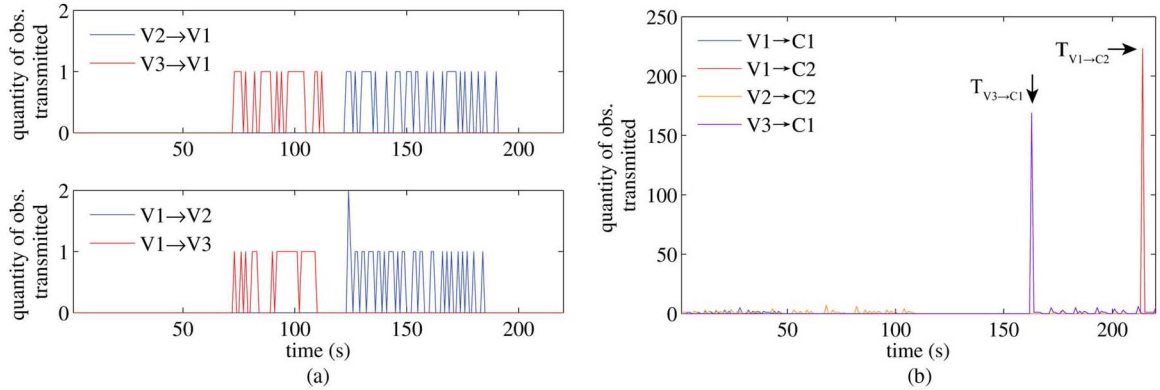

Fig. 12. Communication bandwidth cost in V2V and V2I. (a) V2V communication bandwidth. Vehicles communicate and synchronize position data with each other when in range. (b) V2I communication bandwidth. Vehicles contribute observations to the base station when they are within communication range of a data collection point.

algorithm very close to a solution using full communication coverage.

- increasing the communication range of V2I and/or V2V: to increase time duration that a vehicle stays observable to data collection points and other vehicles.
- optimizing the routes of vehicles: with vehicle density unchanged, an increased frequency of V2V communication could be achieved by planning the vehicles' routes to increase the number of interactions.

The algorithm additionally benefits from a shorter time delay of observations as the computational expense of the algorithm is to some extent determined by the length of *blind time*. The particle filter rewinds back to a historical point once new delayed observations are received; the number of steps to rerun depends on the oldest observation in the received observations set $\mathbf{\Omega}^{v_p}_{k|k-1}$ and are ultimately bounded by the sliding time window size T_w, as previously discussed in Section V-E. All in all, the fundamental idea in optimizing any implementation of the tracking approach proposed in this paper is to minimize the *blind time*.

The V2I bandwidth requirements from the experimental results were dominated by two major transactions illustrated in Fig. 12(b). V3 transmitted 169 absolute position observations at time $T_{\mathrm{V3}\to\mathrm{C1}}$ (162 s) and V1 transmitted 223 observations at $T_{\mathrm{V1}\to\mathrm{C2}}$ (213 s). This was much less than the maximum V2I bandwidth cost predicted by $N_v \tau^{v_p \to I}$. This was because in a large environment, moving vehicles generally

are only in communication range for a relatively short period of time. The observations indirectly collected from other vehicles are transmitted to the base station together with the vehicle's own egocentric observations in a single transaction. The maximum V2I bandwidth cost would be reached in cases where a vehicle is in communication range with another vehicle for a long period before the transaction occurs, as would happen in a parking lot or when vehicles travel close together.

For V2V communication, the bandwidth cost is negligible and is bounded by $N_v - 1$, according to Table IV. In a scenario containing three vehicles, the maximum V2V bandwidth cost is two absolute observations per iteration, as validated by the experimental results shown in Fig. 12(a).

The observation harvesting mechanism substantially increases the robustness of vehicle tracking in large environments with only a small bandwidth cost. A fast network connection time is crucial when a sparse collection of vehicles are moving in a large environment. Communication in a global wireless network can easily be interrupted by vehicle motion, as the signal propagation path between moving vehicles is constantly changing. The observation harvesting approach uses a store-and-synchronize concept to deal with intermittent communication and aims to disseminate data in an opportunistic manner. Without the additional overheads that come with packet routing, the fast and lightweight P2P communication makes the observation harvesting mechanism an effective approach for sharing observations among mobile vehicles and fixed infrastructure in applications where a global network is not feasible.

The main characteristic of observation harvesting is that every vehicle keeps the latest information for as many vehicles as possible in its local observation pool. The temporary failure of some vehicles, or even the majority of vehicles in the network, will not result in the failure of the entire network. This is a particularly attractive characteristic for applications where safety is strongly emphasized.

VII. Conclusion and Future Work

This paper has presented a probabilistic algorithm to track multiple vehicles in a large area with delayed observations. The algorithm is based on a vehicle model that incorporates the properties of the surrounding environment. Environmental properties are built into acceleration, speed, and timing profiles using real historical data collected. The observation harvesting concept is proposed for effective and robust data dissemination among vehicles and fixed infrastructure without requiring global communication. The most informative position information is shared among vehicles moving around a site and forwarded to the base station via returning vehicles. The estimation of vehicle positions relies mainly on the long-term motion prediction algorithm in the base station, when no direct observations are available to reduce the uncertainty of the vehicle position estimate. This paper has presented a particle filter approach capable of dealing with delayed observations. The base station updates vehicle position estimates with absolute position information gathered from returning vehicles, together with V2I observations from fixed data collection points distributed in the area. Negative information is also incorporated at the fusion stage in addition to positive observations.

The results presented in this paper show that it is possible to obtain consistent position estimates for multiple vehicles over long periods of time. V2V communication combined with a limited number of data collection points was used to demonstrate large-scale multiple vehicle tracking without a full coverage communication network. The experimental results clearly showed the improvement from incorporating V2V communication with the modeling constraints and using positive and negative information. This is a significant contribution since it paves the way for the implementation of resource optimization algorithms when full coverage networks are not available or feasible. This facilitates another area of research regarding resource planning incorporating vehicle uncertainty due to discrete positioning information. It is of fundamental importance to optimize the utilization of vehicle resources in industrial applications. Current fleet monitoring and dispatch systems require full network coverage to facilitate the planning of vehicle operations. The algorithm presented in this paper will provide an estimate of vehicle position with associated uncertainty at all times. This will enable the development of a new set of optimization algorithms to implement fleet monitoring and vehicle dispatching without the infrastructure and maintenance expenses of a full coverage communication network.

The future work will focus on cooperative tracking incorporating relative V2V observations, potentially using a mixture of absolute observations and relative distance measurements. In addition, for future work, the optimization of locations for data collection points and other mechanisms for increasing the availability of harvested information will be further examined. This is expected to lead to a reduced or a potentially bounded position estimation error for the fleet of vehicles, which would enable other productivity-related tasks such as dispatching.

References

[1] J. Vreeswijk, M. Mahmod, and B. van Arem, "Energy efficient traffic management and control—The ecomove approach and expected benefits," in *Proc. 13th IEEE Int. Conf. ITSC*, Madeira, Portugal, Sep. 2010, pp. 955–961.

[2] C. Savarese, J. M. Rabaey, and K. Langendoen, "Robust positioning algorithms for distributed ad-hoc wireless sensor networks," in *Proc. Gen. Track Annu. Conf. USENIX ATEC*, 2002, pp. 317–327.

[3] A. Thangavelu, K. Bhuvaneswari, K. Kumar, K. Senthilkumar, and S. N. Sivanandam, "Location identification and vehicle tracking using VANET (VETRAC)," in *Proc. ICSCN*, 2007, pp. 112–116.

[4] E. Yoneki and J. Crowcroft, "Towards data driven declarative networking in delay tolerant networks," in *Proc. 2nd Int. Conf. Distrib. Event Based Syst.*, Rome, Italy, 2008, pp. 1–2.

[5] M. Shan, S. Worrall, and E. Nebot, "Probabilistic long-term vehicle motion prediction and tracking in large environments," *IEEE Trans. Intell. Transport. Syst.*, vol. 14, no. 2, pp. 539–552, Jun. 2013.

[6] G. Agamennoni, J. I. Nieto, and E. M. Nebot, "Estimation of multivehicle dynamics by considering contextual information," *IEEE Trans. Robot.*, vol. 28, no. 4, pp. 855–870, Aug. 2012.

[7] R. Fraile and S. Maybank, "Vehicle trajectory approximation and classification," in *Proc. Brit. Mach. Vis. Conf.*, 1998, pp. 832–840.

[8] M. Bennewitz, W. Burgard, G. Cielniak, and S. Thrun, "Learning motion patterns of people for compliant robot motion," *Int. J. Robot. Res.*, vol. 24, no. 1, pp. 31–48, 2005.

[9] D. Vasquez, T. Fraichard, and C. Laugier, "Incremental learning of statistical motion patterns with growing hidden Markov models," *IEEE Trans. Intell. Transport. Syst.*, vol. 10, no. 3, pp. 403–416, Sep. 2009.
[10] W. Hu, D. Xie, T. Tieniu, and S. Maybank, "Learning activity patterns using fuzzy self-organizing neural network," *IEEE Trans. Syst., Man, Cybern.*, vol. 34, no. 3, pp. 1618–1626, Jun. 2004.
[11] S.-Y. Oh and Y. Yim, "Modelling of vehicle dynamics from real vehicle measurements using a neural network with two-state hybrid learning for accurate long-term prediction," *IEEE Trans. Veh. Technol.*, vol. 53, no. 4, pp. 1076–1084, Jul. 2004.
[12] J. Zhang, F.-Y. Wang, K. Wang, W.-H. Lin, X. Xu, and C. Chen, "Datadriven intelligent transportation systems: A survey," *IEEE Trans. Intell. Transport. Syst.*, vol. 12, no. 4, pp. 1624–1639, Dec. 2011.
[13] H. Wymeersch, J. Lien, and M. Z. Win, "Cooperative localization in wireless networks," *Proc. IEEE*, vol. 97, no. 2, pp. 427–450, Feb. 2009.
[14] H. Wymeersch, U. Ferner, and M. Z. Win, "Cooperative Bayesian self-tracking for wireless networks," *IEEE Commun. Lett.*, vol. 12, no. 7, pp. 505–507, Jul. 2008.
[15] N. Alsindi and K. Pahlavan, "Cooperative localisation bounds for indoor ultra-wideband wireless sensor networks," *EURASIP J. Adv. Signal Process.*, vol. 2008, pp. 852509-1–852509-13, Apr. 2008.
[16] A. Bahr, M. R. Walter, and J. J. Leonard, "Consistent cooperative localisation," in *Proc. IEEE ICRA*, Kobe, Japan, May 2009, pp. 3415–3422.
[17] T. Bailey, M. Bryson, H. Mu, J. Vial, L. McCalman, and H. Durrant-Whyte, "Decentralised cooperative localisation for heterogeneous teams of mobile robots," in *Proc. IEEE ICRA*, Shanghai, China, May 2011, pp. 2859–2865.
[18] N. Patwari, J. N. Ash, S. Kyperountas, A. O. Hero, III, R. L. Moses, and N. S. Correal, "Locating the nodes: Cooperative localisation in wireless sensor networks," *IEEE Signal Process. Mag.*, vol. 22, no. 4, pp. 54–69, Jul. 2005.
[19] R. Madhavan, K. Fregene, and L. E. Parker, "Distributed cooperative outdoor multirobot localisation and mapping," *Auton. Robots*, vol. 17, no. 1, pp. 23–39, Jul. 2004.
[20] E. Adamey and U. Ozguner, "Cooperative multitarget tracking and surveillance with mobile sensing agents: A decentralised approach," in *Proc. 14th IEEE ITSC*, Washington, DC, USA, Oct. 2011, pp. 1916–1922.
[21] S. Worrall and E. M. Nebot, "Using non-parametric filters and sparse observations to localise a fleet of mining vehicles," in *Proc. IEEE ICRA*, Roma, Italy, Apr. 2007, pp. 509–516.
[22] J. Su, J. Scott, P. Hui, J. Crowcroft, E. Lara, C. Diot, A. Goel, M. Lim, and E. Upton, "Haggle: Seamless networking for mobile applications," in *Proc. 9th IEEE Int. Conf. Ubiquitous Comput.*, Innsbruck, Austria, 2007, pp. 391–408.
[23] T. Bailey and H. Durrant-Whyte, Decentralised data fusion with delayed states for consistent inference in mobile ad hoc networks, Australian Centre Field Robot., Univ. Sydney, Sydney, NSW, Australia, Tech. Rep. [Online]. Available: www.personal.acfr.usyd.edu.au/tbailey/papers/delayedstateddf.pdf
[24] H. Mu, T. Bailey, P. Thompson, and H. Durrant-Whyte, "Decentralised solutions to the cooperative multi-platform navigation problem," *IEEE Trans. Aerosp. Electron. Syst.*, vol. 47, no. 2, pp. 1433–1449, Apr. 2011.
[25] J. Capitán, L. Merino, F. Caballero, and A. Ollero, "Delayed-state information filter for cooperative decentralised tracking," in *Proc. IEEE ICRA*, Kobe, Japan, May 2009, pp. 3865–3870.
[26] G. Agamennoni, J. Nieto, and E. M. Nebot, "Mining GPS data for extracting significant places," in *Proc. IEEE ICRA*, 2009, pp. 855–862.
[27] G. Agamennoni, J. Nieto, and E. M. Nebot, "Robust inference of principal road paths for intelligent transportation systems," *IEEE Trans. Intell. Transport. Syst.*, vol. 12, no. 1, pp. 298–308, Mar. 2011.
[28] K. Punithankumar, T. Kirubarajan, and A. Sinha, "Multiple-model probability hypothesis density filter for tracking maneuvering targets," *IEEE Trans. Aerosp. Electron. Syst.*, vol. 44, no. 1, pp. 87–98, Jan. 2008.
[29] D. Svensson and L. Svensson, "A new multiple model filter with switch time conditions," *IEEE Trans. Signal Process.*, vol. 58, no. 1, pp. 11–25, Jan. 2010.
[30] Y. Gu and M. Veloso, "Effective multi-model motion tracking using action models," *Int. J. Robot. Res.*, vol. 28, no. 1, pp. 3–19, Jan. 2009.
[31] C. S. Agate, R. M. Wilkerson, and K. J. Sullivan, "Utilizing negative information to track ground vehicles through move–stop–move cycles," in *Proc. SPIE*, Aug. 2004, vol. 5429, pp. 273–283.
[32] J. Hoffmann, M. Spranger, D. Göhring, and M. Jüngel, "Making use of what you don't see: Negative information in Markov localization," in *Proc. IEEE/RSJ Int. Conf. IROS*, Beijing, China, Aug. 2005, pp. 2947–2952.
[33] N. Patwari and A. Hero, III, "Using proximity and quantized RSS for sensor localization in wireless networks," in *Proc. 2nd Int. ACM Workshop WSNA*, San Diego, CA, USA, Sep. 2003, pp. 20–29.
[34] S. Sivaraman and M. M. Trivedi, "A general active-learning framework for on-road vehicle recognition and tracking," *IEEE Trans. Intell. Transport. Syst.*, vol. 11, no. 2, pp. 267–276, Jun. 2010.
[35] S. Munder, C. Schnörr, and D. M. Gavrila, "Pedestrian detection and tracking using a mixture of view-based shape–texture models," *IEEE Trans. Intell. Transport. Syst.*, vol. 9, no. 2, pp. 333–343, Jun. 2008.
[36] Z. Kim, "Robust lane detection and tracking in challenging scenarios," *IEEE Trans. Intell. Transport. Syst.*, vol. 9, no. 1, pp. 16–26, Mar. 2008.
[37] M. Meuter, A. Kummert, and S. Müller-Schneiders, "3D traffic sign tracking using a particle filter," in *Proc. 11th IEEE Int. Conf. ITSC*, Beijing, China, Oct. 2008, pp. 168–173.
[38] S. Worrall and E. Nebot, "Automated process for generating digitised maps through GPS data compression," in *Proc. ACRA*, Brisbane, Australia, Dec. 2007, pp. 1–6.

Mao Shan (M'12) received the B.S. degree in electrical engineering from Shaanxi University of Science and Technology, Xi'an, China, in 2006 and the M.S. degree in 2009 from The University of Sydney, Sydney, NSW, Australia, in 2009. He is currently working toward the Ph.D. degree at The University of Sydney.

His research interests include autonomous systems and localization and tracking algorithms and applications.

Stewart Worrall (M'08) received the Ph.D. degree from The University of Sydney, Sydney, NSW, Australia, in 2009.

He is currently a Research Associate with the Australian Centre for Field Robotics, The University of Sydney. His research is focused on the study and application of technology for vehicle automation and improving vehicle safety.

Favio Masson (M'03) received the B.S. degree in electrical engineering and the Ph.D. degree from Universidad Nacional del Sur, Bahia Blanca, Argentina.

He is currently a Professor with Universidad Nacional del Sur and a Researcher with the National Scientific and Technical Research Council, Buenos Aires, Argentina. His main research interests are in field robotics automation and sensor networks.

Eduardo Nebot (SM'09) received the B.S. degree in electrical engineering from Universidad Nacional del Sur, Bahia Blanca, Argentina, and the M.S. and Ph.D. degrees from Colorado State University, Fort Collins, CO, USA.

He is currently a Professor with The University of Sydney, Sydney, Australia, where he is also the Director of the Australian Centre for Field Robotics. His main research areas are in field robotics automation and intelligent transport systems. The major impact of his fundamental research is in autonomous system, navigation, and safety.